A&A 618, A56 (2018)
https://doi.org/10.1051/0004-6361/201833480

Astronomy & Astrophysics

Gaia GraL: *Gaia* DR2 gravitational lens systems

II. The known multiply imaged quasars⋆

C. Ducourant[1], O. Wertz[2], A. Krone-Martins[3], R. Teixeira[4], J.-F. Le Campion[1], L. Galluccio[5], J. Klüter[6], L. Delchambre[7], J. Surdej[7], F. Mignard[5], J. Wambsganss[6,9], U. Bastian[6], M. J. Graham[8], S. G. Djorgovski[8], and E. Slezak[5]

[1] Laboratoire d'Astrophysique de Bordeaux, Univ. Bordeaux, CNRS, B18N, allée Geoffroy Saint-Hilaire, 33615 Pessac, France
e-mail: christine.ducourant@u-bordeaux.fr
[2] Argelander-Institut für Astronomie, Universität Bonn, Auf dem Hügel 71, 53121 Bonn, Germany
[3] CENTRA, Faculdade de Ciências, Universidade de Lisboa, Ed. C8, Campo Grande, 1749-016 Lisboa, Portugal
[4] Instituto de Astronomia, Geofísica e Ciências Atmosféricas, Universidade de São Paulo, Rua do Matão, 1226, Cidade Universitária, 05508-900 São Paulo, SP, Brazil
[5] Université Côte d'Azur, Observatoire de la Côte d'Azur, CNRS, Laboratoire Lagrange, Boulevard de l'Observatoire, CS 34229, 06304 Nice, France
[6] Zentrum für Astronomie der Universität Heidelberg, Astronomisches Rechen-Institut, Mönchhofstr. 12-14, 69120 Heidelberg, Germany
[7] Institut d'Astrophysique et de Géophysique, Université de Liège, 19c, Allée du 6 Août, 4000 Liège, Belgium
[8] California Institute of Technology, 1200 E. California Blvd, Pasadena, CA 91125, USA
[9] International Space Science Institute (ISSI), Hallerstraße 6, 3012 Bern, Switzerland

Received 23 May 2018 / Accepted 2 July 2018

ABSTRACT

Context. Thanks to its spatial resolution, the ESA/*Gaia* space mission offers a unique opportunity to discover new multiply imaged quasars and to study the already known lensed systems at sub-milliarcsecond astrometric precisions.
Aims. In this paper, we address the detection of the known multiply imaged quasars from the *Gaia* Data Release 2 (DR2) and determine the astrometric and photometric properties of the individually detected images found in the *Gaia* DR2 catalogue.
Methods. We have compiled an exhaustive list of quasar gravitational lenses from the literature to search for counterparts in the *Gaia* DR2. We then analysed the astrometric and photometric properties of these *Gaia*'s detections. To highlight the tremendous potential of *Gaia* at the sub-milliarcsecond level we finally performed a simple Bayesian modelling of the well-known gravitational lens system HE0435-1223, using *Gaia* DR2 and HST astrometry.
Results. From 481 known multiply imaged quasars, 206 have at least one image found in the *Gaia* DR2. Among the 44 known quadruply imaged quasars of the list, 29 have at least one image in the *Gaia* DR2, 12 of which are fully detected (2MASX J01471020+4630433, HE 0435-1223, SDSS1004+4112, PG1115+080, RXJ1131-1231, 2MASS J11344050-2103230, 2MASS J13102005-1714579, B1422+231, J1606-2333, J1721+8842, WFI2033-4723, WGD2038-4008), eight have three counterparts, eight have two and one has only one. As expected, the modelling of HE0435-1223 shows that the model parameters are significantly better constrained when using *Gaia* astrometry compared to HST astrometry, in particular the relative positions of the background quasar source and the centroid of the deflector. The *Gaia* sub-milliarcsecond astrometry also significantly reduces the parameter correlations.
Conclusions. Besides providing an up-to-date list of multiply imaged quasars and their detection in the *Gaia* DR2, this paper shows that more complex modelling scenarios will certainly benefit from *Gaia* sub-milliarcsecond astrometry.

Key words. gravitational lensing: strong – astrometry

1. Introduction

The ESA/*Gaia* space mission (Gaia Collaboration 2016b) constitutes an exceptional opportunity to characterise and to discover multiply imaged quasars, although this was not put forth as one of the science objectives in the mission proposal. With a spatial resolution of ∼0.18″ *Gaia* is roughly comparable to that of *Hubble* Space Telescope (HST) for this particular feature (e.g. Bellini et al. 2011). However *Gaia* being a scanning mission is unique in providing an all-sky coverage with that angular resolution. Thus, by the final *Gaia* data release (DR), a whole population of such multiply imaged quasars would be revealed, providing an all-sky, and the first of this kind, survey of multiply imaged quasars with well understood source detection biases (e.g. de Bruijne et al. 2015; Arenou et al. 2017, 2018).

Several programmes dedicated to systematic searches for lenses in large astronomical surveys such as SDSS, WISE, DES, PanSTARRS, among others, have been developed in recent years (e.g. More et al. 2016, 2017; Lin et al. 2017; Ostrovski et al. 2018), and many of them rely on supervised

⋆ The table of lenses (confirmed and candidates, detected or not in *Gaia* DR2) is only available at the CDS via anonymous ftp to cdsarc.u-strasbg.fr (130.79.128.5) or via http://cdsarc.u-strasbg.fr/viz-bin/qcat?J/A+A/618/A56. A subset of this table is presented in Table B.1.

machine learning algorithms trained on simulations to handle the large volume of imaging data (e.g. Petrillo et al. 2017; Perreault Levasseur et al. 2017; Hartley et al. 2017; Pourrahmani et al. 2018; Lanusse et al. 2018). Naturally, even if *Gaia* does not provide images of the observed sources, contrary to the previously mentioned surveys, its high angular resolution over the entire sky is a major asset to contribute to the discovery and the study of multiply imaged quasars.

Finet & Surdej (2016) investigate the potential of *Gaia* for gravitational lensing and compared it to the detectability with seeing-limited observations for the same limiting magnitude ($G = 20$). They expect at maximum about ∼1600 multiply imaged quasars with an angular separation large enough to be resolved from the ground in an optimal seeing scenario, while scarcely ∼80 would be composed by more than two images. However, they predict that detections from space are much more encouraging, raising the number of multiply imaged quasars detectable by a *Gaia*-like survey to ∼2900, thanks to the improved resolving power alone.

The first *Gaia* data release (DR1; Gaia Collaboration 2016a), besides providing the best available two-parameter astrometry (positions only) at the epoch of its publication, contained only one G mean magnitude, and it did not reach the effective angular resolution necessary to include most of the multiply imaged quasars. This happened due to data processing issues and final astrometric quality reasons (Fabricius et al. 2016; Arenou et al. 2017). Yet, several multiply imaged quasars discovered from other large surveys such as Pan-STARRS, DES, SDSS-III BOSS, HSCS or VST-ATLAS, were subsequently identified with at least one *Gaia* DR1 detection (e.g. Agnello et al. 2015, 2017, 2018b; Lemon et al. 2017, 2018; Ostrovski et al. 2018).

The *Gaia* DR2 (Gaia Collaboration 2018) on the other hand, starts to deliver colour information and thus to become self-sufficient in the search for new lenses. It also starts to reach effective angular resolutions that are capable of resolving more multiply imaged quasars, expected with typical separations below 1″. The *Gaia* DR2 effective resolution reaches ∼0.4″, with completeness for separations larger than ∼2.2″ (Gaia Collaboration 2018). However this resolution applies strictly only to astrometry and G band photometry; colour data are available for objects with separations down to ∼2″, but its completeness only reaches ∼3.5″ (Gaia Collaboration 2018). Even if it is still far from the ultimate resolving power of the *Gaia* instrument, the *Gaia* DR2 is a significant advance over DR1, as beyond its much improved effective angular resolution, it contains five-parameter astrometric data (positions, proper-motions, parallax) and also colour information for most objects. This significantly simplifies the extraction of genuine extragalactic sources from the galactic stellar contaminants. Only the faintest or most problematic objects are characterised by just a two-parameters solution in this data release, which is unfortunately the case for several multiply imaged quasars as their magnitudes are often close to the *Gaia* limiting sensitivity at (G∼20.7).

As part of a larger effort to discover and study multiply imaged quasar candidates from the various *Gaia* data releases, our group first searched for new lensed systems around known or candidate quasars, enabling the discovery of highly probable multiply imaged quasar candidates for the first time from *Gaia* data alone (*Gaia* GraL Paper I; Krone-Martins et al. 2018). In the present work, we report our findings regarding the identification of known gravitationally lensed quasars in *Gaia* DR2. We have analysed the statistical astrometric properties of the detected lensed images and provide improved relative astrometry for them. We also derive soft astrometric filters that will be applied, as part of a global blind search (*Gaia* GraL Paper III; Delchambre et al., in prep.), to differentiate foreground stars from extragalactic objects without rejecting the faint components of known lensed systems. To illustrate how the exquisite optical astrometry of *Gaia* at the sub-milliarcsecond level may help to better constrain the lenses, we performed a simple modelling of the quadruple lens HE0435-1223 in a Bayesian framework, both using *Gaia* and HST astrometry, for comparison purposes.

The paper is organised as follows: in Sect. 2 we describe the construction of our list of gravitationally lensed quasars and candidates from published data. Sect. 3 presents the matching statistics of this list of known systems with the *Gaia* DR2. Section 4 presents the astrometric properties of the *Gaia* DR2 data for the known systems. A simple modelling within the Bayesian framework of a known lens using *Gaia* DR2 astrometry is described and discussed in Sect. 5. Finally, we summarise our findings in Sect. 6.

2. Compiled list of gravitationally lensed quasars

We have attempted to compile an as-complete-as-possible list of known gravitationally lensed quasars that were published in the literature prior to the *Gaia* DR2, including some recent candidates that are not yet spectroscopically confirmed. The major source of known gravitational lenses included in our list is the CASTLES (CfA-Arizona Space Telescope LEns Survey of gravitational lenses) site (Kochanek et al. 1999)[1] providing information for about 100 lenses, most of them observed with HST. Another important single source of known multiply imaged quasars is the SDSS Quasar Lens Search site (SQLS)[2], aimed to discover lensed quasars from the large homogeneous data of the Sloan Digital Sky Survey (SDSS) providing data on 49 additional lensed systems. We also included several quasar systems from the Master Lens Database (Moustakas 2012)[3], a community-supported compilation of all discovered strong gravitational lenses. Finally we complemented our list with recent and more scattered discoveries from the literature. This list is being kept up-to-date, and will be maintained at least until the final *Gaia* data release. For the sake of completeness, we also included in this list the candidates with indication in the literature of just one image (usually spectroscopic candidates) expecting from the exceptional resolving power of *Gaia* that it may resolve some of them into multiple images in one of its data releases.

Our resulting list of published lensed or lens-candidate quasars contains 481 systems (233 confirmed systems and 248 lensed quasar candidates). This list is only available in electronic form at the CDS, including access through Virtual Observatory ready tools, it comprises lens identifiers, references and the *Gaia* astrometry and photometry when a match was found in the DR2. A subset of our list is presented in Table B.1 (quadruply imaged quasars with at least one detection in the *Gaia* DR2). The summarised statistical properties of our entire list in terms of number of systems with 1, 2, 3, and 4 and more images and status are given in Table 1.

[1] https://www.cfa.harvard.edu/castles/
[2] http://www-utap.phys.s.u-tokyo.ac.jp/~sdss/sqls/lens.html
[3] http://admin.masterlens.org/index.php?

Table 1. Statistics of the known multiply imaged quasars present in our reference list (Col. 2) and of the corresponding detected systems in *Gaia* DR2 (Col. 3).

Lensed images	Number of known lenses	Number detected in *Gaia* DR2
1	55 + (213) = 268	11 + (17) = 28
2	133 + (33) = 166	112 + (32) = 144
3	2 + (1) = 3	4 + (1) = 5
4+	43 + (1) = 44	28 + (1) = 29
Total	233+(248) = 481	155 +(51) = 206

Notes. Col. 1: number of astrometric positions given in the literature. A lensed system is considered to be detected in the *Gaia* DR2 if at least one of its images is detected. Numbers in parentheses correspond to the gravitationally lensed quasar candidates not spectroscopically confirmed yet.

3. Gravitationally lensed quasars in *Gaia* DR2

We extracted sources from the *Gaia* DR2 within a radius of 10″ around each source of our compiled list of known gravitationally lensed quasars using ADQL and the *Gaia* archive facility at ESAC (Salgado et al. 2017). We obtained the positions (α, δ), parallaxes (ϖ), proper-motion components (μ_α, μ_δ) and fluxes in the G, $G_{\rm BP}$ and $G_{\rm RP}$ pass-bands (Evans et al. 2018) along with their respective uncertainties.

For each individual image of each system, we performed a positional cross-match within a maximum angular separation of 0.5″ between the astrometry found in the literature and the *Gaia* DR2. We visually inspected all systems one by one, by comparing the *Gaia* DR2 detections to the system discovery papers and/or archival images from Aladin (Bonnarel et al. 2000; Boch et al. 2014).

Of the 481 gravitational lens systems (including candidates), 206 have at least one image matched with a *Gaia* DR2 source. The overall detection statistics of known systems that result from our examination is given in Table 1. An all-sky chart in galactic coordinates of the known lenses is shown in Fig. 1 along with a specification of the *Gaia* detection.

In Table B.1 we present a subset of our list: the quads for which at least one match was found in the *Gaia* DR2. The complete list of lenses and detection is available in electronic form only at the CDS.

Of the 44 known systems with four images (or more), 29 have at least one image detected in *Gaia* DR2. Within this group, one system has just one image detected, eight have two images, eight have three images and 12 are fully detected with four images seen in the *Gaia* data around the target direction. In Fig. A.1, we provide charts for the 12 systems with four detections with the *Gaia* DR2 positions given relative to the A image (the brightest image in the system discovery pass-band) together with flux ratios. Of those which are fully detected, only five are characterised by sub-milliarcsec astrometry, and are reported in Table 2. The faintest image (in G band) of the others is detected but poorly constrained.

Several quadruply imaged systems were not completely detected, despite the fact that the apparent magnitudes and angular separations of the system images are within *Gaia*'s capabilities. For example, this is the case Q2237+030; only two out of its four known components are published in *Gaia* DR2. The diffraction limited resolving power of the *Gaia* instrument is ∼0.2″, but as commented in Sect. 1, the effective angular resolution of the *Gaia* DR2 is much worse than that, attaining at most ∼0.4″, but with completeness of only ∼2.2″. This loss of resolution restricts the detection of the ∼2900 lenses predicted by Finet & Surdej (2016). This happens for multiple reasons, all of them at the ground processing stage, as the *Gaia* raw data cross-matching, the validation of the astrometric solution and the filtering of possible spurious sources. It is expected, however, that at each *Gaia* data release the effective angular resolution will improve and thus systems with each time smaller angular separations that are not yet separated in the *Gaia* DR2 will be disentangled.

4. Astrometric properties of the *Gaia* DR2 gravitationally lensed quasars

The images of a quasar produced by strong gravitational lensing are peculiar since they are not independent astronomical sources but multiple images of the same source, possibly with part of the host galaxy visible as small segments of an arc. Accordingly, they can produce some particular astrometric signatures in the *Gaia* DR2 solution, that could be helpful to discover further lensed quasar systems in the *Gaia* data.

Of the 382 individual images found in the *Gaia* DR2 coming from the 178 confirmed gravitationally lensed quasars with two or more images, 65 have a *Gaia* two-parameter astrometric solution, that is, right ascension and declination only (see Lindegren et al. 2018 for a description of the *Gaia* DR2 astrometric solution selection). The other 317 images have complete five-parameter solutions $(\alpha, \delta, \mu_\alpha \cos(\delta), \mu_\delta, \varpi)$. We investigated the statistical properties of the *Gaia* DR2 parameters of the multiple images of the known gravitationally lensed quasars, with results shown in Fig. 2. This figure shows that parallaxes and proper motions of the images resulting from lensing occasionally reach large values for sources expected to have neither parallax nor motion. However, this results from the fact that these images are rather faint, at the limit of the *Gaia* DR2 sensitivity where the uncertainties from random noise are also large. In addition it may also be that some images are embedded in extended and diffuse structures.

In a search for multiply imaged quasars in the *Gaia* DR2, applying a straight astrometric filter aiming at excluding stars from the deviation from zero parallaxes and proper motions weighted by the expected uncertainties, would likely also exclude a large number of images of lenses. So, based on the distribution of these parameters for the known lenses, we established the following softer astrometric cuts, that at the expense of a certain level of stellar contamination, avoid the rejection of genuine lens systems or of one or several images within a system.

Gaia DR2 sources that should be accepted in such a search would likely comply with $\varpi - 3\sigma_\varpi < 4$ mas and $|\mu| - 3\sigma_\mu < 4\,\mathrm{mas\,yr^{-1}}$. We note here that μ stands for $\mu_\alpha \cos(\delta)$ and μ_δ.

Indeed, we also adopted these soft filters in *Gaia* GraL Paper I (Krone-Martins et al. 2018), where we presented the first ever discoveries of quadruply imaged quasar candidates from data of an astrometric space mission. These statistical astrometric properties derived from *Gaia* measurements are also being used in a large, machine learning based, systematic blind search for lenses in *Gaia* DR2 (*Gaia* GraL Paper III; Delchambre et al., in prep.).

5. Gravitational lens modelling with sub-mas astrometry

Gravitational lensing provides an efficient tool to explore various aspects of our universe and several of its components. In

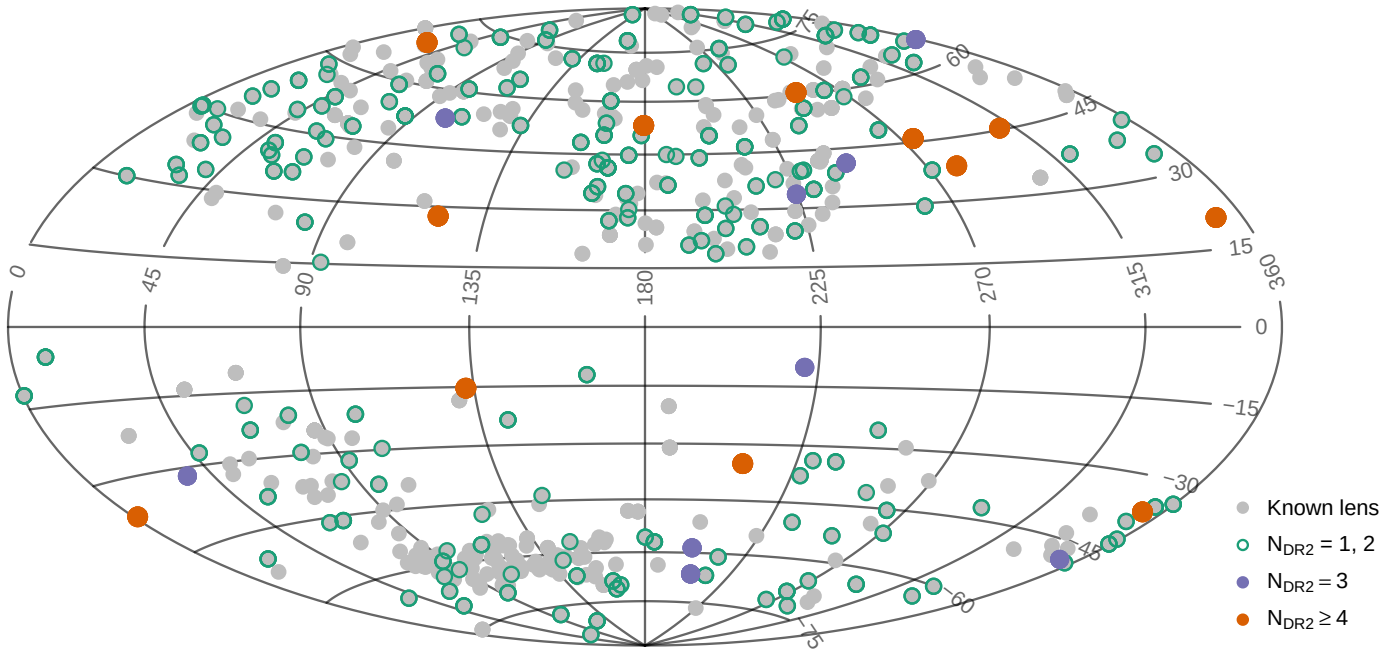

Fig. 1. All-sky chart in galactic coordinates with the galactic anti-centre in the *middle*. The known multiply imaged quasars are indicated in grey. The systems presenting one or two counterparts in *Gaia* DR2 are surrounded by a green open circle. The systems with three *Gaia* DR2 detections are indicated with purple filled circles, while the systems with four or more detections are indicated with orange filled circles.

the strong regime, the inference of physically meaningful quantities from observational data usually requires the accurate modelling of the gravitational potential of the deflector. For example, the ability of modern time-delay cosmography to infer the Hubble constant H_0 with a competitive precision relies significantly on its capacity in dealing with families of degeneracies existing between different plausible lens mass profiles (Saha 2000; Wucknitz 2002; Liesenborgs & De Rijcke 2012; Schneider & Sluse 2013). To probe the deflector mass distribution in the region where multiple images are formed, simple parameterised mass models are commonly used whose parameters are fixed by the observational constraints (e.g. Keeton 2001, 2010; Lefor & Futamase 2014; Lefor 2014), typically the lensed quasar image positions, the morphology of extended components, microlensing-free flux ratios, and time delays between image pairs. Naturally, a better accuracy in the observed parameters leads to a more reliable model. For the five known lenses RXJ1131-1231, SDSS1004+4112, 2MASS J1134-2103, HE0435-1223, and WFI2033-4723, the *Gaia* DR2 provides quasar image position measurements with an unprecedented precision of a few tenths of a milliarcsecond. With an improvement of an order of magnitude over typical HST astrometric accuracy, these new astrometric data should help to better constrain the lens models. Considering four of the five known quadruply imaged quasars reported in Table 2 for which *Gaia* and HST astrometric data are available, the average of the *Gaia* astrometric uncertainties affecting the equatorial coordinates of the four lensed quasar images is found to be 0.43 mas compared to 3.29 mas using the corresponding HST data. This represents a huge gain (by more than a factor 7) in astrometric precision.

In this section, we illustrate how the improved astrometric accuracy obtained with *Gaia* may impact the lens modelling. To this end, we propose to optimise a smooth model to the observed image positions alone, within the Bayesian framework. The idea consists in simultaneously sampling the posterior

Table 2. Relative astrometry for five known quadruply imaged quasars fully detected in the *Gaia* DR2.

Identifier	$\Delta\alpha\cos(\delta)$ (mas)	$\Delta\delta$ (mas)
HE0435-1223		
A	0.0 ± 0.16	0.0 ± 0.14
B	−1476.56 ± 0.19	552.94 ± 0.16
C	−2466.27 ± 0.21	−603.05 ± 0.16
D	−938.66 ± 0.30	−1614.43 ± 0.25
SDSS1004+4112		
A	0.00 ± 0.35	0.00 ± 0.52
B	1315.29 ± 0.36	3531.57 ± 0.49
C	−11039.10 ± 0.47	−4494.69 ± 0.68
D	−8403.23 ± 1.21	9701.47 ± 1.50
RXJ1131-1231		
A	588.68 ± 0.36	1118.89 ± 0.23
B	617.52 ± 0.39	2305.97 ± 0.25
C	0.0 ± 0.47	0.0 ± 0.30
D	−2522.23 ± 1.60	1993.80 ± 0.80
2MASS J1134-2103		
A	0.0 ± 0.11	0.0 ± 0.07
B	729.32 ± 0.11	1755.49 ± 0.07
C	−1947.39 ± 0.11	−772.70 ± 0.07
D	−1247.12 ± 0.28	1366.93 ± 0.20
WFI2033-4723		
A1	−2196.54 ± 0.33	1261.42 ± 0.34
A2	−1483.18 ± 0.26	1375.75 ± 0.30
B	0.0 ± 0.27	0.0 ± 0.24
C	−2113.84 ± 0.33	−277.84 ± 0.32

Notes. The image references have been chosen to match those reported either in https://www.cfa.harvard.edu/castles/ or in their reference papers. They are not necessarily the brightest images in the *Gaia* *G*-band.

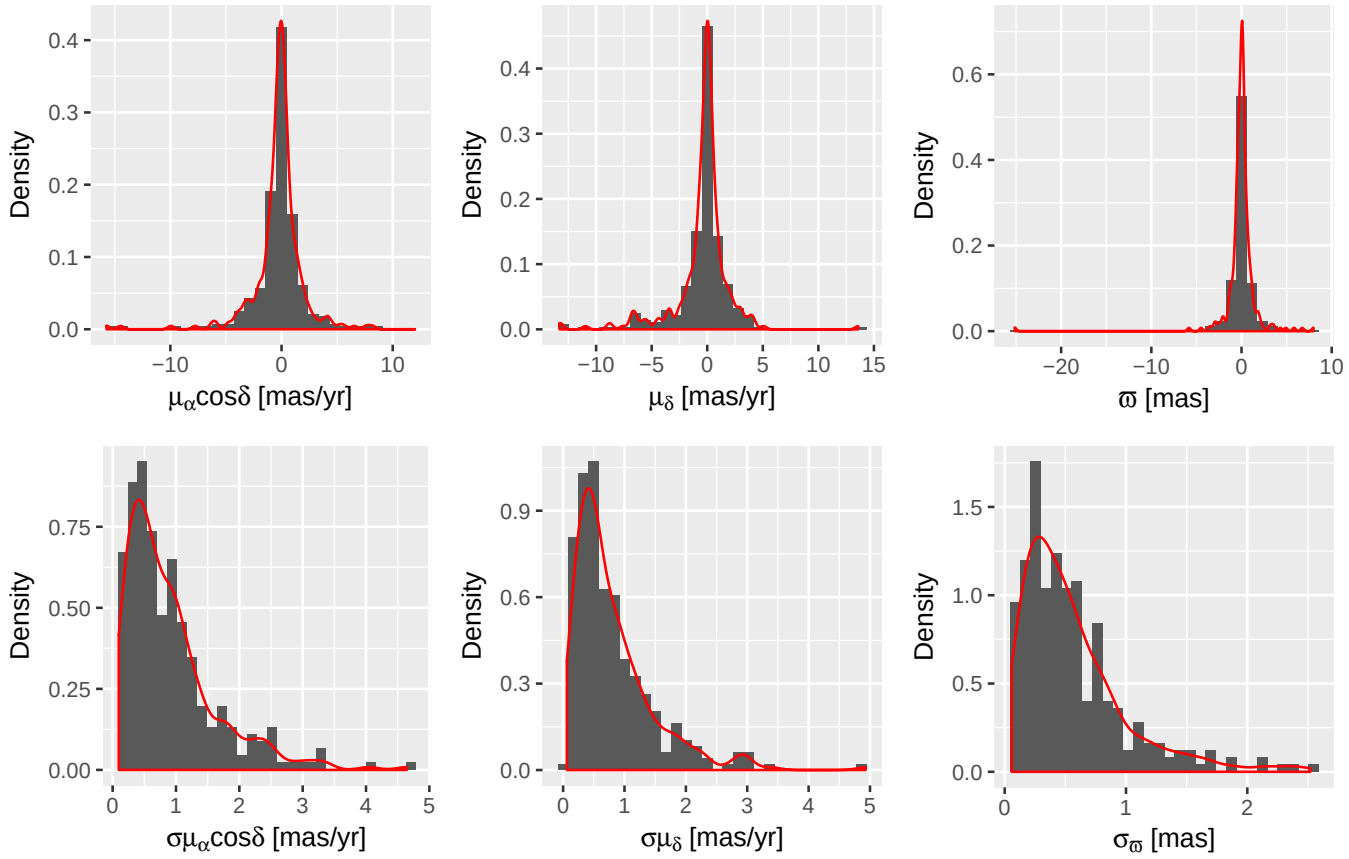

Fig. 2. Distributions of the astrometric parameters and their uncertainties for all the *Gaia* DR2 counterparts of the individual images of known multiply imaged quasars with five parameter astrometric solutions.

probability density functions (PDFs) for all model parameters using a Markov chain Monte Carlo (MCMC) method, and then comparing the PDFs obtained from *Gaia*'s astrometry with the ones derived from the astrometry found in the literature. We want to point out that our objective here is not to construct a set of realistic lens models in the sense that they could be used to perform time delay cosmography. Instead, we have focussed on how *Gaia* astrometric uncertainties may positively affect the goodness of a more complex fit, which would include microlensing-free flux ratios, time delays, non-lensing data related to the main deflector, or even simultaneous reconstruction of the source and deflector surface brightnesses.

We model the main deflector as a singular isothermal ellipsoid (SIE, see e.g. Kormann et al. 1994) which effectively describes the mass distribution of a massive early-type galaxy in the region where multiple images are formed (Gilman et al. 2017). A SIE is characterised by five free parameters; the Einstein radius $\theta_{\rm E}$, the elliptical axes ratio q and position angle θ_q, and the lens centroid $(x_{\rm G}, y_{\rm G})$ with respect to image A. Since the lensed quasar image positions are generally most sensitive to the local mass distribution, we model the large-scale contributions and possible close line-of-sight galaxy perturbing effects with an external shear term (g) characterised by its absolute value γ and position angle θ_γ (see e.g., Kochanek et al. 2006). The resulting SIEg model is thus kept simple, which limits the number of free parameters and avoids the use of the full multi-plane lensing formalism (Schneider 2014; McCully et al. 2014, 2016). In addition, we consider the position of the point-like source (β_x, β_y) with respect to image A that is also free to vary during the optimization process, bringing the number of free parameters n_k to nine.

To draw samples from the posterior PDFs, we used `emcee`[4] (Foreman-Mackey et al. 2013), a python package which implements the affine invariant ensemble sampler for MCMC proposed by Goodman & Weare (2010). Since we only used the lensed image positions $\boldsymbol{\theta}_{\rm obs}$ as observational data to fit, the log-likelihood function simply reads

$$\ln p(\boldsymbol{\theta}_{\rm obs}|\boldsymbol{k}) = -\frac{1}{2}\sum_{j=1}^{2N}\left(\frac{\left(\theta_{{\rm obs},j} - \theta_{{\rm model},j}(\boldsymbol{k})\right)^2}{\sigma^2_{{\rm obs},j}} - \ln\left(\sigma^2_{{\rm obs},j}\right)\right), \quad (1)$$

where $\boldsymbol{k}$ is the vector of free parameters, N the number of lensed images (hence $2N$ constraints), $\sigma_{\rm obs}$ the astrometric uncertainties, and $\boldsymbol{\theta}_{\rm model}(\boldsymbol{k})$ the lensed image positions obtained from the free parameters $\boldsymbol{k}$ and generated with the python package `pySPT`[5] (Wertz & Orthen 2018). To control the sampling, only two hyperparameters need to be tuned: an adjustable scale parameter a and the number $N_{\rm w}$ of walkers. The scale parameter a has a direct impact on the acceptance rate of each walker, namely the ratio of accepted to proposed candidates, and was set to $a = 2$, following Goodman & Weare (2010). A walker can be seen as a Metropolis-Hastings chain (see, e.g., MacKay 2003) whose associated proposal distribution depends on the positions of all the other walkers (Foreman-Mackey et al. 2013). Prior to run the MCMC, we initialised $N_{\rm w} = 350$ walkers in a small n_k-dimensional ball of the parameter space around a highly probable solution, formerly obtained using the public lens modelling

[4] https://github.com/dfm/emcee
[5] https://github.com/owertz/pySPT

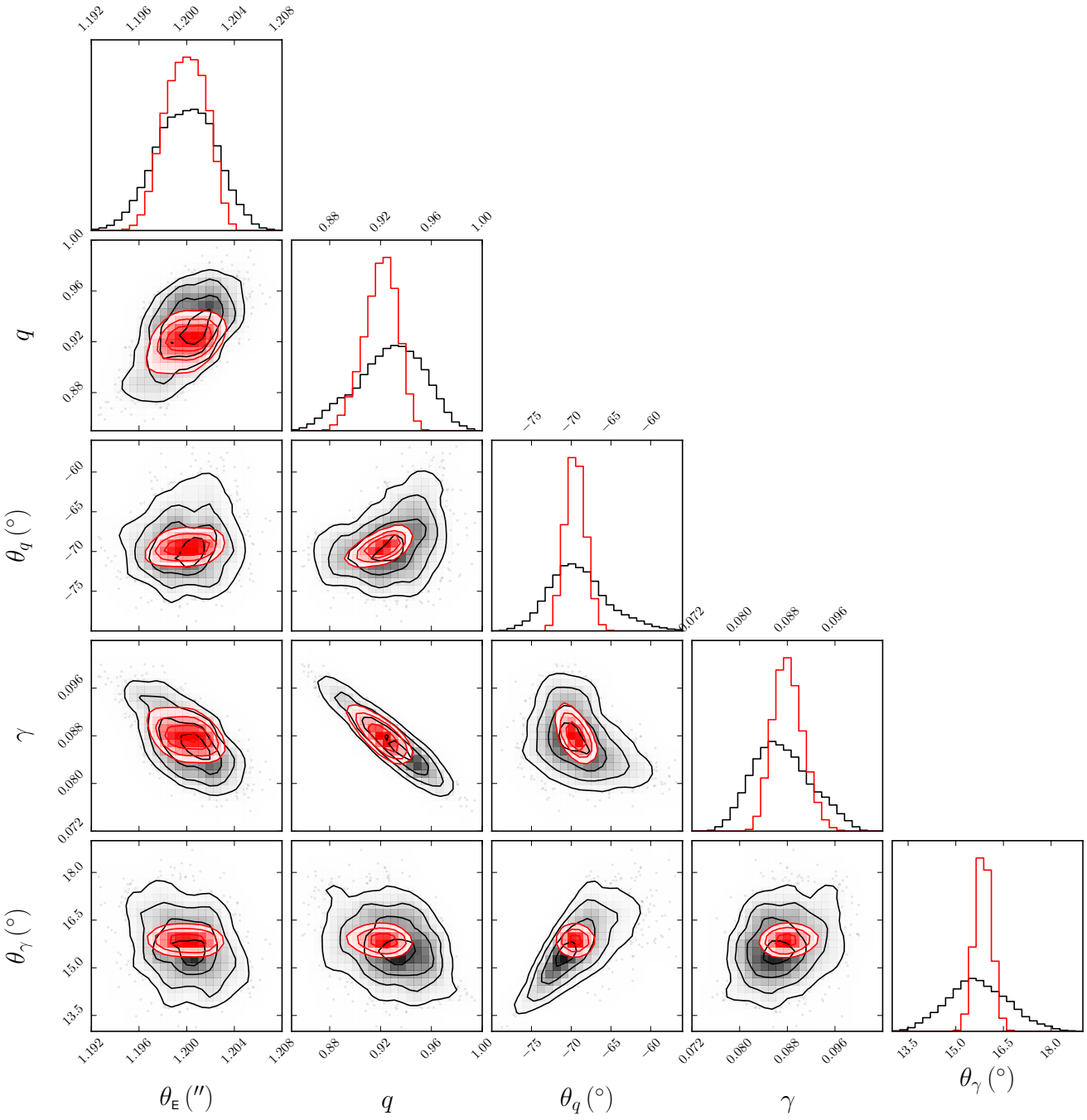

Fig. 3. Results of the MCMC simulations for HE0435-1223, displayed as a corner plot for the five model parameters. Results obtained from *Gaia*'s data are presented in red and with HST data in grey. The diagonal panels illustrate the posterior PDFs while the off-axis panels illustrate the correlation between the parameters. The three inner contours represent the 68.3%, 95.4%, and 99.7% confidence intervals.

code `lensmodel`[6] (v1.99, Keeton 2001). Obviously this initial model may not be the most appropriate one and is more likely a local solution in the parameter space. Nevertheless, it constitutes a valid starting point to illustrate our intention.

The analysis has been performed for the five lenses from Table 2 for which HST image position measurements are available, namely HE0435-1223, SDSS1004+4112, RXJ1131-1231, 2MASS J1134-2103, and WFI2033-4723. In Figs. 3 and 4, we illustrate the MCMC results in the form of corner plots for HE0435-1223, which are representative of each of the five quadruply imaged quasars that we have preliminarily modelled. The HE0435-1223 image positions measured with the Wide Field Camera 3 (IR/F160W, Robberto et al. 2002) mounted on the HST come from Kochanek et al. (2006), showing astrometric uncertainties between 3 and 5 mas. As expected, all the posterior PDFs obtained from the *Gaia* data show narrower widths than those obtained from HST data, while some of them are slightly shifted. Thus the use of *Gaia* astrometry data significantly reduces the ranges of valid model parameters around a highly probable solution, as shown in Table 3. The Einstein radius value has only been slightly improved with respect to HST observations, while the source position is constrained

[6] http://physics.rutgers.edu/~keeton/gravlens/2012WS/

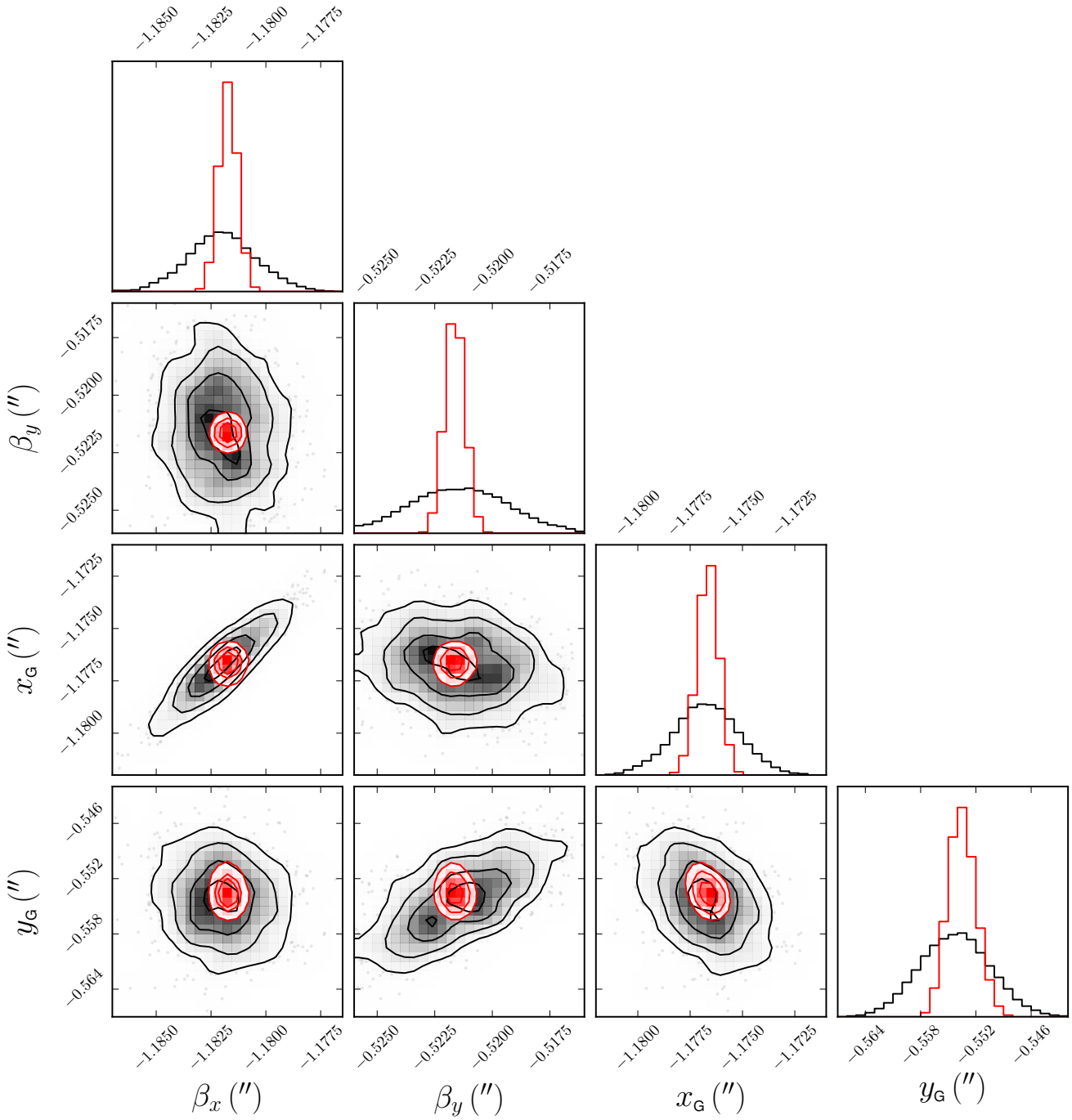

Fig. 4. Results of the MCMC simulations for HE0435-1223, displayed as a corner plot for the source and deflector positions. Results obtained from *Gaia*'s data are presented in red and with HST data in grey. The diagonal panels The diagonal panels illustrate the posterior PDFs while the off-axis panels illustrate the correlation between the parameters. The three inner contours represent the 68.3%, 95.4%, and 99.7% confidence intervals.

within a σ-error ellipse of $(\sigma_{\beta_x}, \sigma_{\beta_y}) = (0.1, 0.1)$ mas. This one order of magnitude improvement indicates that the sub-mas astrometry of *Gaia* clearly helps to better constrain the position of the point-like source as well as the source surface brightness reconstruction as part of a more realistic modelling scenario.

We also note that the *Gaia* DR2 astrometry reduces significantly the resulting correlation structure between the modelled parameters, in comparison with the correlations obtained from the modelling using HST data: the absolute value of the correlation coefficients between θ_q and θ_γ, and θ_q and q, in Fig. 3 and between β_y and y_G, and β_x and x_G in Fig. 4, are clearly reduced thanks to the improved astrometry.

A more advanced version of the lens modelling within the Bayesian framework described in this section will be consistently applied to all the known lenses and to the highly probable lens candidates discovered from a systematic search around quasars (*Gaia* GraL Paper I, Krone-Martins et al. 2018) and from the systematic blind-search for lenses in the entire *Gaia* DR2 (*Gaia* GraL Paper III, Delchambre et al., in prep.), and this will be presented in a forthcoming work (*Gaia* GraL Paper IV, Wertz et al., in prep.).

Table 3. SIEg lens model parameters derived for HE0435-1223.

Parameters	HST	*Gaia*
θ_E ($''$)	1.2 ± 0.003	1.2 ± 0.002
q	0.93 ± 0.03	0.9210 ± 0.01
θ_q (°)	−69.4 ± 3.8	−69.5 ± 0.8
γ	0.087 ± 0.005	0.088 ± 0.002
θ_γ (°)	15.7 ± 0.9	15.9 ± 0.1
β_x (mas)	−1182.0 ± 1.6	−1181.7 ± 0.1
β_y (mas)	−521.4 ± 2.1	−521.6 ± 0.1
x_G (mas)	−1176.7 ± 1.5	−1176.6 ± 0.3
y_G (mas)	−554.2 ± 3.7	−553.6 ± 1.2

Note. The reported values are medians within 1σ error bars.

6. Conclusions

The availability of high-precision and high-accuracy astrometric data as provided by the ESA/*Gaia* space mission opens a new window to detect and model gravitationally lensed quasar systems with an unprecedented refinement. This is bound to impact on fundamental applications in astronomy that are derived from this phenomena, such as the study of the lensing galaxy populations, distant quasars, dark matter and dark energy properties and consequently the determination of cosmological parameters. To exploit this new field with the *Gaia* data, we have set up a collaboration group, the *Gaia* GraL team, to systematically analyse the gravitationally lensed quasar content throughout the *Gaia* data releases. The topics covered include searches for new multiply imaged quasar candidates, identifications of known lenses in the *Gaia* data, modelling of the lenses using the outstanding *Gaia* astrometry and multi-colour photometry, and fostering ground-based follow-up for final confirmation.

In this paper we explain how we first generated an up-to-date list of known gravitationally lensed quasars, including lensed quasars too faint to be observed by *Gaia*. The *Gaia* GraL list of known gravitationally lensed quasars will be kept up-to-date with respect to the astronomical literature at least until the final *Gaia* data release. Each *Gaia* data release will be analysed to verify the detection of known gravitational lenses.

Then we provide here the first ever sub-milliarcsecond astrometric data for hundreds of known gravitationally lensed quasars. The search is based on the aforementioned list matched to the *Gaia* DR2 astrometric catalogue, the largest and most precise astrometric reference available to date. Our lens results bring almost one order of magnitude improvement in astrometric precision compared to a typical HST observation. Moreover, even if *Gaia* DR2 is still an early data release lacking many lensed images, it brings high-precision astrometry complemented with photometric data for most known lensed systems. Thus, it provides a glimpse of the content that will become available in the forthcoming *Gaia* data releases.

Of the 481 presently known or candidate gravitationally lensed quasars, we have found in the *Gaia* DR2 at least one counterpart for 206 of them. From these objects, the quadruply-imaged quasars occupy a specially relevant place, as they provide the more stringent physical parameter inferences. There are 44 presently known quads. From these, 29 have been found with at least one entry in *Gaia* DR2 and 12 of them are fully detected with all four images. As the images of many of these objects have smaller angular separations than the *Gaia* DR2 effective angular resolution, we expect the forthcoming data releases to provide information for most images with separations down to ∼0.18″, as the *Gaia* releases gradually reach the instrument spatial resolution. We also provide *Gaia* DR2 astrometric and photometric data for all known lenses to date.

Finally, we show that the adoption of high-precision astrometry from *Gaia* DR2 to model the well-known lens system HE0435-1223 results in a significant improvement in constraining the lens parameters of a SIEg model around a highly probable solution, and that it also significantly reduces the model parameter correlations, in comparison to standard HST astrometry. Such constraints will certainly be further improved with the increased precision of forthcoming *Gaia* nominal mission data releases, expected for 2020 (DR3) and 2022 (DR4), and the still to be announced data release(s) of the *Gaia* mission extension.

As a final conclusion this work vividly demonstrates the significant impact of high-precision astrometry from *Gaia* and future mission concepts as the JASMINE series (Gouda 2011), GaiaNIR (Hobbs et al. 2016), and Theia (The Theia Collaboration et al. 2017), to the study of strong gravitational lensing. This paper also exemplifies the ever wider impact of astrometry and of the *Gaia* satellite, pushing its limits from its original goal of studying the Milky Way galaxy towards more distant extragalactic sources and associated phenomena.

Acknowledgements. The authors wish to thank the referee for his constructive comments. AKM acknowledges the support from the Portuguese Fundação para a Ciência e a Tecnologia (FCT) through grants SFRH/BPD/74697/2010, from the Portuguese Strategic Programme UID/FIS/00099/2013 for CENTRA, from the ESA contract AO/1-7836/14/NL/HB and from the Caltech Division of Physics, Mathematics and Astronomy for hosting a research leave during 2017-2018, when this paper was prepared. LD and JS acknowledge support from the ESA PRODEX Programme "*Gaia*-DPAC QSOs" and from the Belgian Federal Science Policy Office. OW acknowledges support from a fellowship for Post-doctoral Researchers by the Alexander von Humboldt Foundation. SGD and MJG acknowledge a partial support from the NSF grants AST-1413600 and AST-1518308, and the NASA grant 16-ADAP16-0232. We acknowledge partial support from "Actions sur projet INSU-PNGRAM", and from the Brazil-France exchange programmes Fundação de Amparo à Pesquisa do Estado de São Paulo (FAPESP) and Coordenação de Aperfeiçoamento de Pessoal de Nível Superior (CAPES) – Comité Français d'Évaluation de la Coopération Universitaire et Scientifique avec le Brésil (COFECUB). The authors wish to thank C. Spindola Duarte for her help with the source referencing. This work has made use of the computing facilities of the Laboratory of Astroinformatics (IAG/USP, NAT/Unicsul), whose purchase was made possible by the Brazilian agency FAPESP (grant 2009/54006-4) and the INCT-A, and we thank the entire LAi team, specially Carlos Paladini, Ulisses Manzo Castello, and Alex Carciofi for the support. This research has made use of the VizieR catalogue access tool, CDS, Strasbourg, France. The original description of the VizieR service was published in A&AS 143, 23. This research has made use of 'Aladin sky atlas' developed at CDS, Strasbourg Observatory, France. This work has made use of results from the ESA space mission *Gaia*, the data from which were processed by the *Gaia* Data Processing and Analysis Consortium (DPAC). Funding for the DPAC has been provided by national institutions, in particular the institutions participating in the *Gaia* Multilateral Agreement. The *Gaia* mission website is: `http://www.cosmos.esa.int/gaia`. Some of the authors are members of the *Gaia* Data Processing and Analysis Consortium (DPAC).

References

Agnello, A., Kelly, B. C., Treu, T., & Marshall, P. J. 2015, MNRAS, 448, 1446
Agnello, A., Lin, H., & Kuropatkin, N. 2017, MNRAS, in press
Agnello, A., Grillo, C., Jones, T., et al. 2018a, MNRAS, 474, 3391
Agnello, A., Schechter, P. L., Morgan, N. D., et al. 2018b, MNRAS, 475, 2086
Anguita, T., Faure, C., Kneib, J.-P., et al. 2009, A&A, 507, 35
Aravena, M., Spilker, J. S., Bethermin, M., et al. 2016, MNRAS, 457, 4406
Arenou, F., Luri, X., Babusiaux, C., et al. 2017, A&A, 599, A50
Arenou, F., Luri, X., Babusiaux, C., et al. 2018, A&A, 616, A17
Bade, N., Siebert, J., Lopez, S., Voges, W., & Reimers, D. 1997, A&A, 317, L13
Bellini, A., Anderson, J., & Bedin, L. R. 2011, PASP, 123, 622
Berghea, C. T., Nelson, G. J., Rusu, C. E., Keeton, C. R., & Dudik, R. P. 2017, ApJ, 844, 90
Biggs, A. D., Rusin, D., Browne, I. W. A., et al. 2003, MNRAS, 338, 1084
Blackburne, J. A., Wisotzki, L., & Schechter, P. L. 2008, AJ, 135, 374

Boch, T., & Fernique, P. 2014, in Astronomical Data Analysis Software and Systems XXIII, eds. N. Manset, & P. Forshay, ASp Conf. Ser., 485, 277
Bolton, A. S., Moustakas, L. A., Stern, D., et al. 2006, ApJ, 646, L45
Bonnarel, F., Fernique, P., Bienaymé, O., et al. 2000, A&AS, 143, 33
Bordoloi, R., Rigby, J. R., Tumlinson, J., et al. 2016, MNRAS, 458, 1891
Dahle, H., Gladders, M. D., Sharon, K., et al. 2013, ApJ, 773, 146
de Bruijne, J. H. J., Allen, M., Azaz, S., et al. 2015, A&A, 576, A74
Eigenbrod, A., Courbin, F., Meylan, G., Vuissoz, C., & Magain, P. 2006, A&A, 451, 759
Evans, D. W., Riello, M., De Angeli, F. 2018, A&A, 616, A4
Fabricius, C., Bastian, U., Portell, J. et al. 2016, A&A, 595, A3
Falco, E. E., Kochanek, C. S., Lehar, J. 1999, ArXiv e-prints [arXiv:astro-ph/9910025]
Finet, F., & Surdej, J. 2016, A&A, 590, A42
Foreman-Mackey, D., Hogg, D. W., Lang, D., & Goodman, J. 2013, PASP, 125, 306
Gaia Collaboration (Brown, A. G. A., et al.) 2016a, A&A, 595, A2
Gaia Collaboration (Prusti, T., et al.) 2016b, A&A, 595, A1
Gaia Collaboration (Brown, A.) 2018, A&A, 616, A1
Ghosh, K. K., & Narasimha, D. 2009, ApJ, 692, 694
Gilman, D., Agnello, A., Treu, T., Keeton, C. R., & Nierenberg, A. M. 2017, MNRAS, 467, 3970
Goicoechea, L. J., & Shalyapin, V. N. 2016, A&A, 596, A77
Goodman, J., & Weare, J. 2010, Commun. Appl. Math. Comput. Sci., 5, 65
Gouda, N. 2011, Scholarpedia, 6, 12021
Hartley, P., Flamary, R., Jackson, N., Tagore, A. S., & Metcalf, R. B. 2017, MNRAS, 471, 3378
Hobbs, D., Høg, E., & Mora, A. 2016, ArXiv e-prints [arXiv: 1609.07325].
Huchra, J., Gorenstein, M., Kent, S., et al. 1985, AJ, 90, 691
Inada, N., Becker, R.H., & Burles, S. 2003a, AJ, 126, 666
Inada, N., Oguri, M., Pindor, B., et al. 2003b, Nature, 426, 810
Inada, N., Burles, S., Gregg, M. D., et al. 2005, AJ, 130, 1967
Inada, N., Oguri, M., Becker, R. H., et al. 2006, AJ, 131, 1934
Inada, N., Oguri, M., Becker, R. H., et al. 2007, AJ, 133, 206
Inada, N., Oguri, M., Shin, M.-S., et al. 2010, AJ, 140, 403
Inada, N., Oguri, M., Shin, M.-S., et al. 2012, AJ, 143, 119
Inada, N., Oguri, M., Rusu, C. E., Kayo, I., & Morokuma, T. 2014, AJ, 147, 153
Jackson, N. 2008, MNRAS, 389, 1311
Jackson, N., Rampadarath, H., Ofek, E. O., Oguri, M., & Shin, M.-S. 2012, MNRAS, 419, 2014
Johnston, D. E., Richards, G. T., Frieman, J. A., et al. 2003, AJ, 126, 2281
Keeton, C. R., 2001, ApJ, submitted [arXiv:astro-ph/0102340]
Keeton, C. R. 2010, Gen. Relativ. Gravit., 42, 2151
Kochanek, C. S. 2006, Gravitational Lensing: Strong, Weak and Micro, eds. G. Meylan, P. Jetzer, P. North, et al. Saas-Fee Advanced Course 33, 91
Kochanek, C. S., Falco, E. E., & Impey, C. D. 1999, in After the Dark Ages: When Galaxies were Young, eds. S. Holt, & E. Smith, AIP Conf. Ser., 470, 163
Kochanek, C. S., Morgan, N. D., Falco, E. E., et al. 2006, ApJ, 640, 47
Kormann, R., Schneider, P., & Bartelmann, M. 1994, A&A, 284, 285
Kostrzewa-Rutkowska, Z., Kozłowski, S., Lemon, C., et al. 2018, MNRAS, 476, 663
Krone-Martins, A., Delchambre, L., & Wertz, O. 2018, A&A, 616, L11 (Paper I)
Lanusse, F., Ma, Q., Li, N., et al. 2018, MNRAS, 473, 3895
Leethochawalit, N., Jones, T. A., Ellis, R. S., et al. 2016, ApJ, 820, 84
Lefor, A. T. 2014, Astron. Comput., 5, 28
Lefor, A. T., & Futamase, T. 2014, Astron. Comput., 6, 28
Lemon, C. A., Auger, M. W., McMahon, R. G., & Koposov, S. E. 2017, MNRAS, 472, 5023
Lemon, C. A., Auger, M. W., McMahon, R. G., & Ostrovski, F. 2018, MNRAS, 479, 5060
Liesenborgs, J., & De Rijcke, S. 2012, MNRAS, 425, 1772
Limousin, M., Richard, J., Jullo, E., et al. 2016, A&A, 588, A99
Lin, H., Buckley-Geer, E., Agnello, A., et al. 2017, ApJ, 838, L15
Lindegren, L., Hernandez, J., & Bombrun, A. 2018, A&A, 616, A2
Lucey, J. R., Schechter, P. L., Smith, R. J., & Anguita, T. 2018, MNRAS, 476, 927
MacKay, D.J. 2003, Information Theory, Inference and Learning Algorithms (Cambridge University Press)
Magain, P., Surdej, J., Swings, J.-P., Borgeest, U., & Kayser, R. 1988, Nature, 334, 325
McCully, C., Keeton, C. R., Wong, K. C., & Zabludoff, A. I. 2014, MNRAS, 443, 3631
McCully, C., Keeton, C. R., Wong, K. C., & Zabludoff, A. I. 2016, in American Astronomical Society Meeting Abstracts, Vol. 227, 338, 02
McKean, J. P., Browne, I. W. A., Jackson, N. J., et al. 2005, MNRAS, 356, 1009
Meyer, R. A., Delubac, T., Kneib, J. P., & Courbin, F. 2017, A&A, submitted [arXiv:1711.01184]
More, A., Oguri, M., Kayo, I., et al. 2016, MNRAS, 456, 1595
More, A., Lee, C.-H., Oguri, M., et al. 2017, MNRAS, 465, 2411
Morgan, N. D., Snyder, J. A., & Reens, L. H. 2003, AJ, 126, 2145
Morgan, N. D., Caldwell, J. A. R., Schechter, P. L., et al. 2004, AJ, 127, 2617
Morokuma, T., Inada, N., Oguri, M., et al. 2007, AJ, 133, 214
Moustakas, L. 2012, The Master Lens Database and The Orphan Lenses Project, HST Proposal
Nayyeri, H., Keele, M., Cooray, A., et al. 2016, ApJ, 823, 17
Oguri, M., Inada, N., Hennawi, J. F., et al. 2005, ApJ, 622, 106
Ostrovski, F., McMahon, R. G., Connolly, A. J., et al. 2017, MNRAS, 465, 4325
Ostrovski, F., Lemon, C. A., Auger, M. W., et al. 2018, MNRAS, 473, L116
Parry, W. G., Grillo, C., Mercurio, A., et al. 2016, MNRAS, 458, 1493
Patnaik, A. R., Browne, I. W. A., Walsh, D., Chaffee, F. H., & Foltz, C. B. 1992, MNRAS, 259, 1P
Perreault Levasseur, L., Hezaveh, Y. D., & Wechsler, R.H. 2017, ApJ, 850, L7
Petrillo, C. E., Tortora, C., Chatterjee, S., et al. 2017, MNRAS, 472, 1129
Pindor, B., Eisenstein, D. J., Inada, N., et al. 2004, AJ, 127, 1318
Pourrahmani, M., Nayyeri, H., & Cooray, A. 2018, ApJ, 856, 68
Reimers, D., Hagen, H.-J., Baade, R., Lopez, S., & Tytler, D. 2002, A&A, 382, L26
Robberto, M., Hanley, C., Dashevsky, I., 2002, The reference pixels on the WFC3 IR detectors, Tech. Rep.
Rusu, C. E., Oguri, M., Minowa, Y., et al. 2016, MNRAS, 458, 2
Rusu, C. E., Berghea, C. T., & Fassnacht, C.D. 2018, MNRAS, submitted [arXiv:1803.07175]
Saha, P. 2000, AJ, 120, 1654
Salgado, J., González-Núñez, J., Gutiérrez-Sánchez, R., et al. 2017, Astronomy and Computing, 21, 22
Schechter, P. L., Morgan, N. D., Chehade, B., et al. 2017, AJ, 153, 219
Schechter, P. L., Anguita, T., Morgan, N. D., Read, M., & Shanks, T. 2018, Res. Notes AAS, 2, 21
Schneider, P. 2014, A&A, 568, L2
Schneider, P., & Sluse, D. 2013, A&A, 559, A37
Sergeyev, A. V., Zheleznyak, A. P., Shalyapin, V. N., & Goicoechea, L. J. 2016, MNRAS, 456, 1948
Shu, Y., Brownstein, J. R., Bolton, A. S., et al. 2017, ApJ, 851, 48
Sluse, D., Surdej, J., Claeskens, J.-F., et al. 2003, A&A, 406, L43
The Theia Collaboration (Boehm, C., et al.) 2017, ArXiv e-prints [arXiv:1707.01348]
Wertz, O., & Orthen, B. 2018, ArXiv e-prints [arXiv: 1801.04151]
Weymann, R. J., Chaffee, F. H., Jr., Davis, M., et al. 1979, ApJ, 233, L43
Williams, P. R., Agnello, A., Treu, T., et al. 2018, MNRAS, 477, L70
Wisotzki, L., Christlieb, N., Liu, M. C., et al. 1999, A&A, 348, L41
Wisotzki, L., Schechter, P. L., Bradt, H. V., Heinmüller, J., & Reimers, D. 2002, A&A, 395, 17
Wisotzki, L., Schechter, P. L., Chen, H.-W., et al. 2004, A&A, 419, L31
Wucknitz, O. 2002, MNRAS, 332, 951

Appendix A: *Gaia* DR2 finding charts of known and confirmed quadruply-imaged quasars

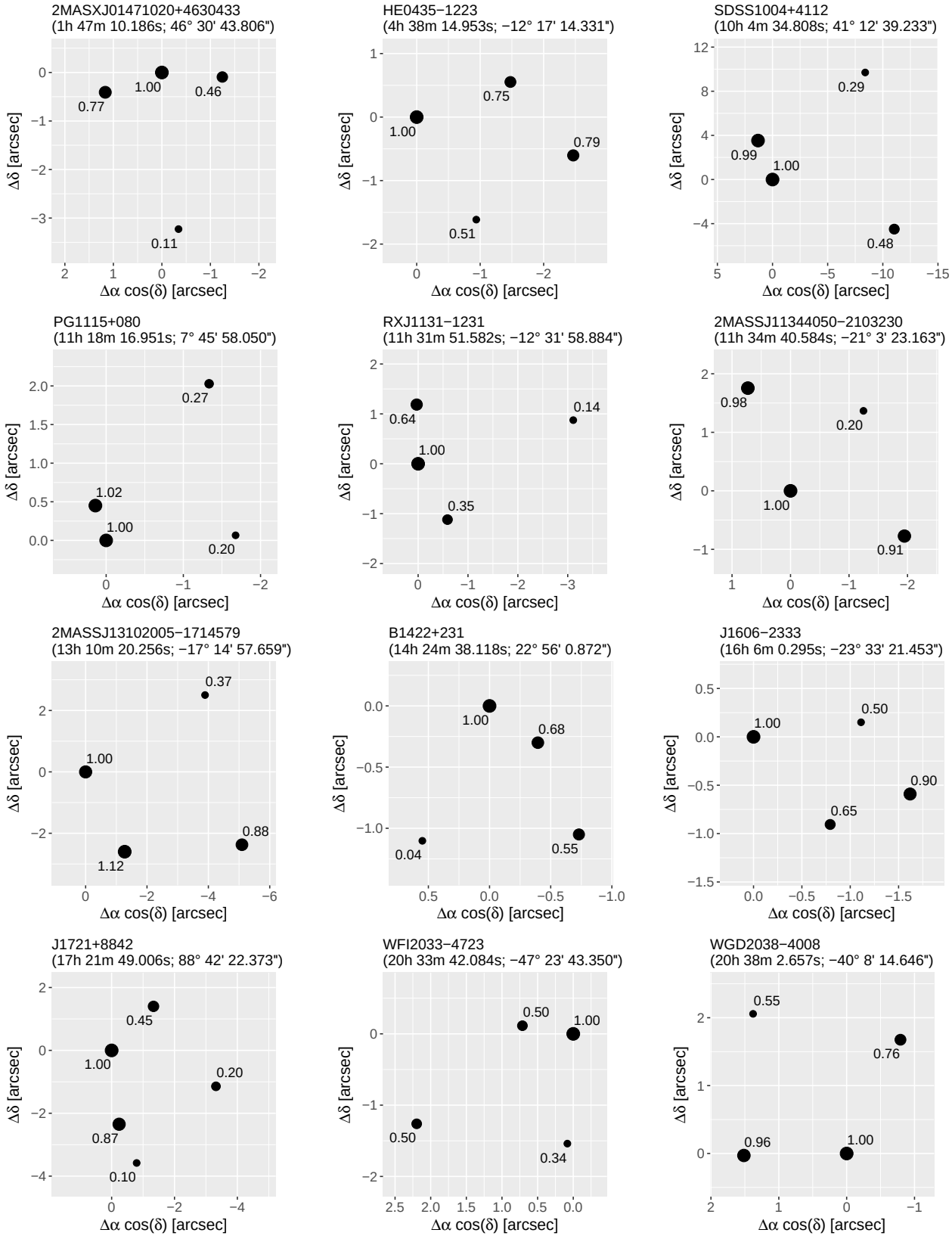

Fig. A.1. Finding charts for the known GLs with four counterparts in the *Gaia* DR2. *Gaia* DR2 astrometry relative to the brightest image (A image) based on the original system discovery data is indicated by black points (except WGD2038-4008, see footnote in Table B.1). The numbers near each image, and the image size, indicate the flux ratios to the brightest image in the original system discovery data. We note that in some cases this may not be the brightest image detected by *Gaia* and therefore generates some flux ratios >1. North is up, east is left.

Appendix B

Table B.1. List of known quadruply-imaged quasars with at least one match in the *Gaia* DR2.

Name	ref	*Gaia* DR2 Source Id	Right ascension (°) ± (mas)	Declination (°) ± (mas)	G (mag)	G_{BP} (mag)	G_{RP} (mag)
2MASX J01471020+4630433 B	19	350937280925970432	26.79193807656 ± 0.1330	46.51214243036 ± 0.2039	16.7405 ± 0.0031		
2MASX J01471020+4630433 D	19	350937280925971456	26.79230269485 ± 0.2699	46.51127175724 ± 0.3121	18.2644 ± 0.0026	18.3850 ± 0.1694	17.5129 ± 0.0107
2MASX J01471020+4630433 A	19	350937280928094336	26.79244106590 ± 0.4754	46.51216827296 ± 0.4487	15.8931 ± 0.0075	15.5900 ± 0.0548	14.8218 ± 0.0441
2MASX J01471020+4630433 C	19	350937280925970304	26.79291224025 ± 4.7897	46.51205497601 ± 2.3003	16.1790 ± 0.0067		
HE0230-2130 B	06	5126705515510051584	38.13811782066 ± 0.2498	−21.29074906026 ± 0.4626	19.3041 ± 0.0078		
HE0230-2130 A	06	5126705515511054080	38.13832537061 ± 0.1989	−21.29067749450 ± 0.3369	19.0355 ± 0.0047	18.3755 ± 0.0226	17.7388 ± 0.0336
HE0230-2130 C	06	5126705515510051712	38.13847486587 ± 0.4449	−21.29024032275 ± 0.6378	20.0651 ± 0.0141		
WISE 025942.9-163543 C	22	5153828508862118912	44.92836484851 ± 0.9512	−16.59520492683 ± 0.6912	20.1708 ± 0.0225		
WISE 025942.9-163543 B	22	5153828504567283072	44.92869905654 ± 0.5370	−16.59511750800 ± 0.4263	19.6393 ± 0.0131		
WISE 025942.9-163543 A	22	5153828508862119040	44.92879162716 ± 0.5258	−16.59536150645 ± 0.4166	19.4150 ± 0.0084	18.9059 ± 0.0573	17.6442 ± 0.0325
J0408-5354 C[a]	18	4779903605191703296	62.09056074627 ± 3.5274	−53.89942733757 ± 2.5860	20.8249 ± 0.0222		
J0408-5354 B[a]	18	4779902849277205760	62.09142458061 ± 0.5550	−53.90025030949 ± 0.5666	20.4514 ± 0.0101	20.2464 ± 0.0971	19.6238 ± 0.0610
J0408-5354 A[a]	18	4779903605192400000	62.08965552446 ± 0.3402	−53.89973595868 ± 0.3595	19.7447 ± 0.0071	19.7080 ± 0.0480	18.7889 ± 0.0462
HE0435-1223 C	08	3178020716638059136	69.56160351805 ± 0.1802	−12.28748166882 ± 0.1294	18.8373 ± 0.0067	18.5996 ± 0.0952	17.8801 ± 0.0610
HE0435-1223 B	08	3178020716640423680	69.56188488232 ± 0.1534	−12.28716055854 ± 0.1249	18.8942 ± 0.0104		
HE0435-1223 D	08	3178020716638059392	69.56203780095 ± 0.2818	−12.28776263363 ± 0.2298	19.3013 ± 0.0104		
HE0435-1223 A	08	3178020716638059264	69.56230465346 ± 0.1145	−12.28731415348 ± 0.0978	18.5754 ± 0.0060	18.0642 ± 0.0452	17.6339 ± 0.0220
J0630-1201 C	23	3000185396723852416	97.53784635400 ± 1.6412	−12.02241686045 ± 2.1094	20.0917 ± 0.0083	19.5704 ± 0.2020	18.4840 ± 0.0277
J0630-1201 A	23	3000185396729743104	97.53799106290 ± 0.8450	−12.02225598303 ± 1.0049	19.9856 ± 0.0067	19.5925 ± 0.0622	18.1779 ± 0.0373
J0630-1201 B	23	3000185396723852544	97.53808564125 ± 0.5711	−12.02194351373 ± 0.6697	20.0078 ± 0.0071	19.2062 ± 0.1361	18.0411 ± 0.0467
HS0810+2554 A	09	682614034415644032	123.38030267112 ± 0.6695	25.75086095081 ± 0.4691	16.1001 ± 0.0062	16.1982 ± 0.0176	15.1723 ± 0.0078
HS0810+2554 D	09	682614034415644160	123.38049319374 ±54.2925	25.75102468034 ±36.3600	18.9633 ± 0.0116		
RXJ0911+0551 D	05	580537088586198656	137.86423190910 ± 0.6464	5.84851723352 ± 0.4200	19.8927 ± 0.0085	19.8129 ± 0.0927	19.1918 ± 0.1998
RXJ0911+0551 C	05	580537092879166720	137.86506252061 ±48.4513	5.84856614310 ±21.7528	19.7670 ± 0.0157		
RXJ0911+0551 B	05	580537092879166848	137.86513579392 ± 0.5169	5.84840999370 ± 0.5057	18.7832 ± 0.0120	18.3875 ± 0.0383	17.8027 ± 0.0263
SDSS0924+0219 A	10	3844748070752040576	141.23256103405 ± 0.2185	2.32371368311 ± 0.2048	18.3811 ± 0.0141	18.3105 ± 0.0502	17.6076 ± 0.05273
SDSS0924+0219 B	10	3844748075046370688	141.23257901195 ± 0.5972	2.32321168663 ± 0.6246	19.9453 ± 0.0145		
SDSS1004+4112 C	11	806853174702355072	151.14095539984 ± 0.3976	41.20964940678 ± 0.5731	19.9953 ± 0.0087	19.8931 ± 0.0883	19.3598 ± 0.0514
SDSS1004+4112 D	11	806853174702356352	151.14192866068 ± 1.1881	41.21359278404 ± 1.4523	20.5619 ± 0.0130	20.2623 ± 0.2021	19.6826 ± 0.0808
SDSS1004+4112 A	11	806853178999388928	151.14503143567 ± 0.2471	41.21089793234 ± 0.3646	19.2071 ± 0.0067	19.3055 ± 0.0434	18.6081 ± 0.0268
SDSS1004+4112 B	11	806853174703246208	151.14551708801 ± 0.2596	41.21187892534 ± 0.3323	19.2223 ± 0.0075	19.2207 ± 0.0422	18.7456 ± 0.0579
J1059+0622 B	25	3864688543049876352	164.86009927358 ±20.6717	6.37436101583 ± 5.3105	17.9809 ± 0.0079		
J1059+0622 A	25	3864688543050432640	164.86015324956 ± 1.3350	6.37420550875 ± 1.4962	17.3898 ± 0.0238	17.2033 ± 0.0118	16.5761 ± 0.0121
HE1113-0641 B	14	3783971985705433984	169.09802843301 ± 6.0376	−6.96068252038 ± 1.8016	17.4980 ± 0.0266	16.7641 ± 0.0348	16.3431 ± 0.0227
HE1113-0641 A	14	3783971985705434112	169.09816765399 ± 7.0797	−6.96080328592 ± 5.1159	17.3972 ± 0.0137	16.8367 ± 0.0507	16.4789 ± 0.0240
PG1115+080 B	01	3817878828361980160	169.57015797740 ± 0.4371	7.76614341006 ± 0.2882	18.9413 ± 0.0109		
PG1115+080 A2	01	3817878828361980544	169.57066712476 ± 0.3243	7.76625027119 ± 0.3194	17.1502 ± 0.0146	16.5405 ± 0.0126	15.9208 ± 0.0158
PG1115+080 C	01	3817878828361980288	169.57025413596 ± 0.3157	7.76668844843 ± 0.1872	18.5837 ± 0.0070	18.5038 ± 0.0603	17.8989 ± 0.0371
PG1115+080 A1	01	3817878828362669568	169.57062805579 ±24.4805	7.76612506243 ± 2.9684	17.1702 ± 0.0110	16.5525 ± 0.0223	15.9258 ± 0.0007

Notes. (1) Name, (2) ref – bibliographic reference (* designates candidates), (3) *Gaia* DR2 Source Id, (4,5) ICRS positions from *Gaia* DR2 at epoch 2015. 5,(6,7,8) *Gaia* G, G_{BP}, G_{RP} magnitudes and standard errors (calculated by CDS). [(a)]J0408-5354 : the images (A, B, C) have been attributed following increasing G mag, and not following Lin et al. (2017). [(b)]J1721+8842 E? : faint extra source detected by *Gaia* DR2 with a two parameters solution astrometry. [(c)]WGD2038-4008 : the images (A, B, C, D) have been attributed following increasing G mag, and not following Agnello et al. (2017) since even considering the photometric data from the aforementioned paper this would not follow the increasing flux order.

References. (01) Weymann et al. (1979), (02) Huchra et al. (1985), (03) Magain et al. (1988), (04) Patnaik et al. (1992), (05) Bade et al. (1997), (06) Wisotzki et al. (1999), (07) Kochanek et al. (1999), (08) Wisotzki et al. (2002), (09) Reimers et al. (2002), (10) Inada et al. (2003a), (11) Inada et al. (2003b), (12) Sluse et al. (2003), (13) Morgan et al. (2004), (14) Blackburne et al. (2008), (15) Inada et al. (2012), (16) Rusu et al. (2016), (17) Sergeyev et al. (2016), (18) Lin et al. (2017), (19) Berghea et al. (2017), (20) Agnello et al. (2017), (21) Agnello et al. (2017), (22) Schechter et al. (2017), (23) Lemon et al. (2018), (24) Lucey et al. (2018), (25) Lemon et al. (2018), (26) Rusu et al. (2018), (27) Falco et al. (1999). References for full table available only at CDS: Morgan et al. (2003, 2004), Johnston et al. (2003), Biggs et al. (2003), Inada et al. (2003b, 2005, 2006, 2007, 2010, 2012, 2014), Wisotzki et al. (2004), Pindor et al. (2004), Oguri et al. (2005), McKean et al. (2005), Eigenbrod et al. (2006), Bolton et al. (2006), Morokuma et al. (2007), Blackburne et al. (2008), Jackson (2008), Anguita et al. (2009), Ghosh & Narasimha (2009), Jackson et al. (2012), Dahle et al. (2013), Limousin et al. (2016), Goicoechea & Shalyapin (2016), Leethochawalit et al. (2016), Nayyeri et al. (2016), More et al. (2016, 2017), Sergeyev et al. (2016), Aravena et al. (2016), Rusu et al. (2016, 2018), Parry et al. (2016), Bordoloi et al. (2016), Shu et al. (2017), Schechter et al. (2017, 2018), Berghea et al. (2017), Ostrovski et al. (2017), Meyer et al. (2017), Lemon et al. (2017, 2018), Agnello et al. (2017, 2018a,b), Kostrzewa-Rutkowska et al. (2018), Lucey et al. (2018), Williams et al. (2018).

Table B.1. continued.

Name	ref	*Gaia* DR2 Source Id	Right ascension [°] ± [mas]	Declination [°] ± [mas]	G [mag]	G_{BP} [mag]	G_{RP} [mag]
RXJ1131-1231 D	12	3586098513051815680	172.96404170566 ± 1.5657	−12.53278020998 ± 0.7744	19.9911 ± 0.0199		
RXJ1131-1231 C	12	3586098513051815808	172.96475942625 ± 0.3308	−12.53333404411 ± 0.2114	19.0189 ± 0.0141		
RXJ1131-1231 A	12	3586098513053631232	172.96492693884 ± 0.1390	−12.53302324209 ± 0.0957	17.8773 ± 0.0149	17.1130 ± 0.0505	16.5723 ± 0.0442
RXJ1131-1231 B	12	3586098508760213248	172.96493514624 ± 0.2091	−12.53269349597 ± 0.1275	18.3639 ± 0.0190		
2MASS J11344050-2103230 C	24	3541826024526317312	173.66852228570 ± 0.0768	−21.05664892265 ± 0.0510	17.2709 ± 0.0045	17.4714 ± 0.0083	16.6770 ± 0.0627
2MASS J11344050-2103230 D	24	3541826024524572288	173.66873072407 ± 0.2741	−21.05605458128 ± 0.1929	18.9371 ± 0.0061		
2MASS J11344050-2103230 A	24	3541826024524572544	173.66910193174 ± 0.0759	−21.05643428362 ± 0.0506	17.1731 ± 0.0049	16.8891 ± 0.0443	16.2567 ± 0.0323
2MASS J11344050-2103230 B	24	3541826024526317568	173.66931901612 ± 0.0764	−21.05594664876 ± 0.0502	17.1949 ± 0.0040	17.1767 ± 0.0759	16.4024 ± 0.0313
SDSS1138+0314 A	27	3800591477621812096	174.51563277165 ± 1.9150	3.24934233962 ± 0.8549	19.6834 ± 0.0104	19.0469 ± 0.0387	18.4332 ± 0.0394
SDSSJ125107.57+293540.5 A	15	1464911708560136064	192.78156710722 ± 0.3323	29.59454644305 ± 0.2214	18.9284 ± 0.0123	18.5397 ± 0.0371	17.8071 ± 0.0252
SDSSJ125107.57+293540.5 B	15	1464911712855560960	192.78169178055 ±33.1507	29.59464933771 ± 4.9416	20.1848 ± 0.0255		
2MASS J13102005-1714579 D	24	3511426761399393152	197.58291817500 ± 0.7841	−17.25000870310 ± 0.6438	20.0227 ± 0.0126	19.8397 ± 0.1231	18.9536 ± 0.0674
2MASS J13102005-1714579 C	24	3511426761399771776	197.58326799853 ± 7.3493	−17.24865451177 ± 3.8113	20.9737 ± 0.0417		
2MASS J13102005-1714579 B	24	3511426761399393280	197.58402962359 ± 0.7657	−17.25007184536 ± 0.4609	19.7662 ± 0.0084	19.5670 ± 0.0685	18.5691 ± 0.0525
2MASS J13102005-1714579 A	24	3511426761399556352	197.58440002563 ± 0.6212	−17.24934978580 ± 0.4847	19.8902 ± 0.0080	19.7893 ± 0.0433	19.0017 ± 0.0435
SDSS J1330+1810 C	16	3746665350016537088	202.57739723361 ± 0.6044	18.17590345192 ± 0.3528	20.0199 ± 0.0097		
SDSS J1330+1810 AB	16	3746665345725273472	202.57776001721 ± 0.8522	18.17557927148 ± 0.5600	18.9459 ± 0.0045	18.5218 ± 0.0191	17.6031 ± 0.0119
H1413+117 C	03	1225461582386033536	213.94255533517 ± 9.6306	11.49554421221 ± 4.0495	17.5918 ± 0.0096		
H1413+117 A	03	1225461582386571008	213.94261368056 ± 1.7339	11.49530779513 ± 1.6421	17.3422 ± 0.0127	16.7056 ± 0.0129	15.9767 ± 0.0151
H1413+117 B	03	1225461582386033792	213.94281630572 ± 1.4809	11.49537124845 ± 1.7926	17.4443 ± 0.0161	17.0120 ± 0.1567	16.1650 ± 0.1682
B1422+231 C	04	1254357435158834560	216.15860664841 ± 0.0877	22.93328372661 ± 0.1121	16.8977 ± 0.0036		
B1422+231 B	04	1254357435159465088	216.15870787479 ± 0.9361	22.93349211808 ± 1.2745	16.6783 ± 0.0021		
B1422+231 A	04	1254357435158834688	216.15882701471 ± 0.5497	22.93357549720 ± 0.6104	16.2555 ± 0.0080	15.987 ± 0.017	14.962 ± 0.011
B1422+231 D	04	1254357435158834816	216.15899268510 ±58.4203	22.93326929457 ±34.3890	19.7110 ± 0.0149		
SDSS J1433+6007 C	21	1618050348046583680	218.34457378805 ± 0.7581	60.12083308456 ± 1.0440	20.2585 ± 0.0117		
SDSS J1433+6007 A	21	1618050348048027648	218.34499683862 ± 0.4977	60.12038164197 ± 0.4310	19.8749 ± 0.0076	19.6307 ± 0.0682	19.1394 ± 0.0539
SDSS J1433+6007 B	21	1618050554206457984	218.34499742143 ± 0.6334	60.12142437659 ± 0.5872	19.9861 ± 0.0094	19.8346 ± 0.0989	19.3034 ± 0.0479
J1606-2333 C	25	6242307087212540160	241.50098822162 ±17.8936	−23.55621065040 ±13.6665	19.3273 ± 0.0097		
J1606-2333 D	25	6242307087220282624	241.50089149589 ±43.2108	−23.55591724742 ± 7.8737	19.6110 ± 0.0163		
J1606-2333 A	25	6242307087212540032	241.50122837627 ± 0.4723	−23.55595910220 ± 0.1969	18.8525 ± 0.0053	18.2655 ± 0.0383	17.5597 ± 0.0275
J1606-2333 B	25	6242307087212539776	241.50073780328 ± 1.3337	−23.55612324162 ± 0.3274	18.9721 ± 0.0115	18.3351 ± 0.0536	17.5623 ± 0.0797
J1721+8842 D	25	1729026461820249728	260.41335642070 ± 0.6103	88.70589729174 ± 0.4895	19.9265 ± 0.0072		
J1721+8842 B	25	1729026466114871424	260.43780732365 ± 0.2382	88.70660390446 ± 0.2481	19.0310 ± 0.0050		
J1721+8842 E?[b]	25	1729026466114871296	260.44440309955 ± 3.4388	88.70521994925 ± 1.0992	20.6595 ± 0.0174		
J1721+8842 A	25	1729026466116588544	260.45419370846 ± 0.1206	88.70621468902 ± 0.1300	18.1755 ± 0.0053	18.3643 ± 0.0387	17.1173 ± 0.0174
J1721+8842 C	25	1729026461820390400	260.45126749084 ± 0.1535	88.70556237840 ± 0.1721	18.3287 ± 0.0084	18.4834 ± 0.0811	17.3640 ± 0.0401
WFI2026-4536 B	13	6675746940384195456	306.54348562606 ± 0.3228	−45.60718787581 ± 0.2604	18.6226 ± 0.0079		
WFI2026-4536 A	13	6675746940384195200	306.54363561758 ± 3.0726	−45.60752504082 ± 1.6543	17.1982 ± 0.0132	16.8025 ± 0.0290	16.2132 ± 0.0125
WFI2033-4723 A1	13	6674418764699092736	308.42535000446 ± 0.2748	−47.39537499737 ± 0.2933	18.0677 ± 0.0071	17.7333 ± 0.0173	17.0862 ± 0.0127
WFI2033-4723 C	13	6674418764698005248	308.42538394120 ± 0.2748	−47.39580256979 ± 0.2726	19.2447 ± 0.0092		
WFI2033-4723 A2	13	6674418764698005376	308.42564273060 ± 0.1850	−47.39534323862 ± 0.2475	18.8196 ± 0.0050		
WFI2033-4723 B	13	6674418764698004992	308.42625134682 ± 0.1890	−47.39572539107 ± 0.1672	18.8262 ± 0.0023	18.7933 ± 0.0767	18.1817 ± 0.0680
WGD2038-4008 C[c]	20	6681326549578891648	309.51078424930 ± 0.5758	−40.13693605210 ± 0.4304	19.9010 ± 0.0055		
WGD2038-4008 A[c]	20	6681326549580116864	309.51107237693 ± 0.5785	−40.13740161713 ± 0.5994	19.6071 ± 0.0095	18.9346 ± 0.1256	17.3375 ± 0.0376
WGD2038-4008 D[c]	20	6681326549578891392	309.51157347188 ± 2.1359	−40.13683014244 ± 1.7719	20.2563 ± 0.0144		
WGD2038-4008 B[c]	20	6681326549578891520	309.51162267018 ± 0.5164	−40.13740966159 ± 0.4163	19.6480 ± 0.0053		
PS1 J205143-111444 A	26*	6901910950299842688	312.93087874749 ± 0.5607	−11.24562339171 ± 0.3446	19.6632 ± 0.0052	19.2664 ± 0.0422	18.5697 ± 0.0377
PS1 J205143-111444 B	26*	6901910950301201024	312.93122111259 ± 0.5220	−11.24509460838 ± 0.2868	19.9321 ± 0.0055	19.9348 ± 0.1826	18.8598 ± 0.0397
PS1 J205143-111444 C	26*	6901910950299842560	312.93160192750 ± 1.5900	−11.24505252971 ± 1.4157	20.7426 ± 0.0163		
Q2237+030 B	02	2704542594213521664	340.12576696218 ± 0.5140	3.35881124314 ± 0.4528	17.6672 ± 0.0097		
Q2237+030 A	02	2704542589921820288	340.12595348968 ± 0.3627	3.35834194908 ± 0.2799	16.7356 ± 0.0109	16.2755 ± 0.0423	15.1978 ± 0.0306